Characterization of Elastic Tensors of Crustal Rocks with respect to Seismic Anisotropy

Anissha Raju

Department of Geological Sciences

University of Colorado, Boulder

Defense Date:

April 5th, 2017

Thesis Advisor

Assoc. Prof. Dr. Kevin Mahan, Department of Geological Sciences

Thesis Committee

Dr. Vera Schulte-Pelkum, Department of Geological Sciences

Prof. Dr. Charles Stern, Department of Geological Sciences

Dr. Daniel Jones, Honors Program

ACKNOWLEDGEMENTS

I would like to thank Dr. Kevin Mahan and Dr. Vera Schulte-Pelkum for overseeing this thesis and initiating a seismic anisotropy reading seminar. Both have been very supportive towards my academic development and have provided endless guidance and support even prior to starting this thesis. Huge thanks to Dr. Charles Stern and Dr. Daniel Jones for serving on the committee and for their excellent academic instruction. Dr. Charles Stern has also been a big part of my academic career. I sincerely appreciate Dr. Sarah Brownlee for allowing me to use her MATLAB decomposition code and her contributions in finding trends in my plots. Thanks to Phil Orlandini for helping me out with generating MTEX plots. Special thanks to all the authors (listed in Appendix A) for providing me their sample elastic stiffness tensors and allowing it to be used in this study. I would also like to express my gratitude to Undergraduate Research Opportunity Program (UROP) of University of Colorado Boulder for partly funding this study. Last but not least, I would like to thank my family and friends for being supportive throughout my undergraduate journey.

TABLE OF CONTENTS

ACKNOWLEDGEMENTS **2**

ABSTRACT **4**

INTRODUCTION **5**

ELASTIC TENSOR DATABASE **9**

METHODS AND ANALYSIS **11**

RESULTS AND DISCUSSION **14**

Anisotropy symmetry 15

Mineralogical trends 18

CONCLUSIONS **22**

REFERENCES **23**

APPENDIX A **26**

ABSTRACT

A wide range of minerals are stable is the Earth's crust. Minerals belong to one of the seven crystal systems and have a wide range of densities. Hence, evaluating crustal seismic anisotropy is very complicated. Seismic anisotropy does not only depend on the types of minerals present, but rather considers mineral orientation, which is greatly dependent on the presence of Lattice Preferred Orientation (LPO), within a rock body. This study aims to investigate mineralogical role in rocks' anisotropy and anisotropy symmetry. Hence, over 100 elastic tensors of crustal rocks was compiled from published studies from all over the world, along with the composition, pressure and temperature conditions of the rock samples. These compiled rock samples are representative of the rock types seen in the lower crust. The elastic tensors were decomposed into different symmetry classes and η_K was calculated for each rock sample. η_K measures the deviation from a perfectly elliptical hexagonal phase velocity. The total rock anisotropy of these samples ranges from 1.27% to 25.47%. Some rock samples dominantly have hexagonal symmetry, while others have orthorhombic and lower symmetry class. Higher amounts of mica in rock samples correlate to a higher hexagonal component of anisotropy. Similarly, rock samples with higher amphibole content tends to have a higher orthorhombic component of anisotropy. It is also shown that rock samples with higher anisotropy have lower η_K value, majority of which are below 1. These trends will be useful in forward modelling studies involving crustal anisotropy.

INTRODUCTION

Incorporation of seismic anisotropy into velocity models is necessary to have a better understanding of the geodynamic development of continents. The effects of anisotropy can also be used to explain the propagation of seismic waves inside the Earth. Other applications of anisotropy studies include: investigating earthquake processes, exploration geophysics, and providing useful insights into processes involved in mountain building (Margheriti et al., 1997). Seismic anisotropy has also been used as a potential explanation for the reflectivity pattern observed from deeper crustal levels (Weiss et al., 1999).

Seismic anisotropy refers to the variation of seismic wave speed as a function of direction of propagation, polarization direction, or both (Eaton and Jones, 2006). As a wave propagates through a single mineral crystal, the wave will travel at the same speed in any direction if the crystal is isotropic (axes are perpendicular to each other and have the same length). However, when waves travel in an anisotropic crystal, the speed of the wave will vary based on the orientation of the crystal due to the variation of elastic constants within the crystal. The wave's speed also changes with the mineral it propagates through due to the mineral symmetry and the density of the mineral. It gets more complex when waves propagate through a rock. This is because a rock is an aggregate of more than one crystal of either one or more than one mineral, and preferred mineral alignment also plays a huge role in controlling the wave speed. Therefore, the Earth's crust is known to be anisotropic due to the variation of rock type and the alignment of minerals in the crust.

Given the fact that a wide range of minerals are stable in the Earth's crust, and minerals can belong to any one of the seven crystal symmetry classes and have a wide range of densities, it is extremely complicated to analyze the Earth's anisotropy. On a larger scale, for example, where sampling paths of teleseismic waves are 100's of km through the Earth, it may be acceptable to consider the crust as isotropic, with the assumption that the various mineral orientations and compositions will balance each

other out, although parts of the mantle are known to have crystal alignment even on that scale. However, at seismic scales of 10's of km or less where only near receiver lithospheric or crustal signals are used, this assumption no longer holds. When taking anisotropy into account, many studies assume hexagonal symmetry, the next highest symmetry and the simplest case after isotropic, for their calculations (Babuska and Cara, 1991).

The elastic tensor of a rock is a multi-dimensional array of numerical values that relates stiffness to the strain of the rock forming minerals. It consists of up to 21 independent coefficients depending on the crystal symmetry (Babuska and Cara, 1991). Hexagonal symmetry needs at least 5 independent elastic coefficients (A, C, F, L and N in the convention introduced by Love, 1944) to describe the elastic tensor. This number increases as the mineral gets less symmetric; up to 21 independent elastic coefficients for a monoclinic symmetry system. Hexagonal symmetry, often known as transversely isotropic (TI) in the seismological literature, is widely used in seismological research due to its simplicity (minimal number of unknown parameters). In a TI body, the elastic properties are invariant when rotated perpendicularly along the axis of symmetry (Babuska and Cara, 1991; Bostock and Christensen, 2012; Porter et al, 2011).

The tensors can be represented in the form of stereonet plots using the MTEX software developed by Hielscher and Schaeben (2008) and Bachmann et al. (2010). A stereonet projection is a lower hemisphere graph of a 3D phase velocity, which in this context, is a visualization of a wave's velocity as it propagates through a rock in various directions. These plots reflect a main anisotropy symmetry exhibited by the rock sample along with the anisotropy of the rock sample. The plots below serve as an example of hexagonal and orthorhombic cases. For an isotropic sample, the P-wave velocity (Vp) is invariant in any direction of propagation, hence the plot will be filled with a single color. In the case of a hexagonal symmetry, there is a fast axis (Figure 1a) with a slower plane perpendicular to it, or a slow axis (Figure 1b) with a faster plane. The fast or slow axes are dependent on whether the axis of symmetry has higher velocity than the plane perpendicular to it (fast axis symmetry) or the axis has slower velocity than the orthogonal plane (slow axis symmetry). Figure 1c depicts a typical orthorhombic system. With the

orthorhombic system, the velocity varies in three different directions; in the orientations displayed in Figure 1, they are in and out, horizontally across and vertically across the stereonet.

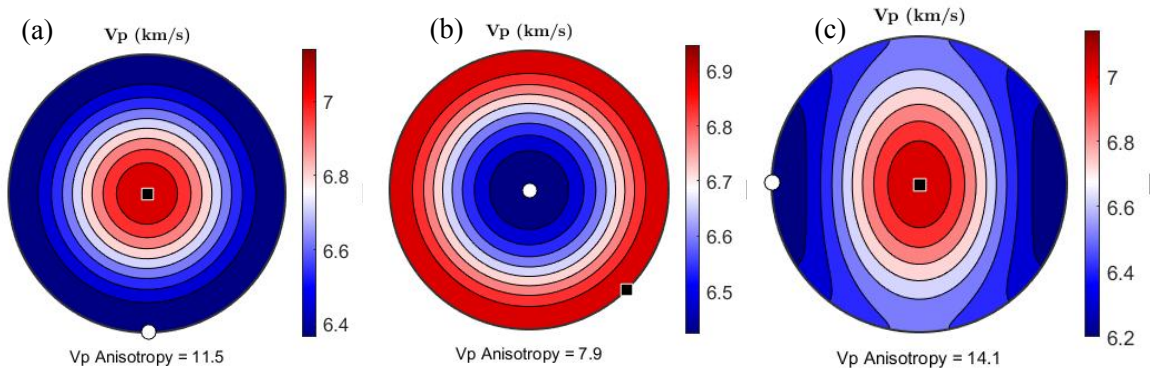

Figure 1: Stereonet projections of fast axis hexagonal(a), slow axis hexagonal (b) and orthorhombic (c) rock sample. The symmetry axis for these stereonet plots are in and out of the stereonet.

Deformation in the crust can cause the minerals to develop a lattice preferred orientation (LPO) and research has shown that LPO has a strong influence on the elastic tensor of the rock (Lloyd and Kendall, 2005). Therefore, the most anisotropic rocks in the crust are metamorphic rocks, which are commonly found in regionally deformed orogens and in shear zones. Mica is an abundant mineral in the continental crust. It tends to align parallel to the shear plane given sufficient strain during deformation events. Hence, a significant number of studies (Weiss et al., 1999; Mahan, 2006; Dempsey et al., 2011) have emphasized mica to evaluate crustal anisotropy. It is important to understand that although minerals have their own crystal symmetry, they could exhibit other types of anisotropy. For example, micas are monoclinic but exhibit hexagonal seismic anisotropy (Alexandrov and Ryzhova (1961) *in* Babuska and Cara, 1991; Porter et al., 2011). It is also due to this reason that a lot of studies have suggested that hexagonal symmetry is sufficient to describe the properties of significant zones of crustal anisotropy (Levin and Park, 1997; Weiss et al., 1999; Godfrey et al., 2000; Porter et al., 2011).

Another common mineral in the lower crust is amphibole. Amphibole, also an anisotropic mineral, tends to develop LPO in shear zones and contributes to crustal anisotropy (Tatham et al., 2008). As amphibole crystals grow, they can crystallize into either monoclinic or orthorhombic crystal systems depending on the type of amphibole. Ji et al. (2015) suggests that amphiboles exhibit orthorhombic anisotropy. Orthorhombic symmetry is the most symmetric class after hexagonal, hence at least nine independent elastic coefficients are needed to describe this symmetry (Babuska and Cara, 1991).

Ward et al. (2012) also looked at the role of quartz in anisotropy by looking at the interference of mica and quartz in mylonites. This study showed that mica is not the only mineral that is responsible for seismic anisotropy and quartz, in fact, reduces the total anisotropy of mylonite as it interferes with mica. Ji et al. (2015) also found that variance of a rock from TI is caused by the presence of quartz along with a few other minerals such as amphibole and sillimanite. Effects of quartz on seismic anisotropy are also dependent with the prevailing slip system and the volume fraction (Ji et al., 2015).

All these recent studies that explored the roles of minerals other than mica in seismic anisotropy are the motivation of this study to further correlate mineral composition to the type of seismic anisotropy beyond the typical mica. This study aims to determine if there is a significant relationship between a few minerals such as quartz, mica and amphibole to an appropriate symmetry. To make this evaluation, an extensive database of elastic tensors is needed to find trends that might have not been investigated or to correct current misconceptions. For this study, I compiled elastic tensors of rocks from existing studies on crustal anisotropy. These tensors are decomposed into their symmetry components and through collection of P-T conditions and composition of the rocks, some general characterizations and trends are found. Using these trends and characterizations helps us understand the observed crustal deformation. Porter et al. (2011) suggested that although the use of receiver functions to examine crustal anisotropy could provide relevant information on deformation history, one major limitation for this technique is the applicability of simplifying geological assumptions. In fact, this is true for all other techniques as well. Thus, having a

central database is crucial. With an extensive database, simplifications of geological assumptions could be reduced or simply wouldn't be necessary anymore.

ELASTIC TENSOR DATABASE

This database includes elastic stiffness tensors from existing literature on seismic anisotropy studies from the year 1993 to the present. No constraints are placed on the tensor data based on their location, rock types or measurement methods of these tensors, except that the collection avoids samples that are anisotropic due to microcracks (shallow crust). In fact, a variation of tensor data is important to build a comprehensive database and to avoid sampling bias. Figure 2 shows the location of the samples in the database. Table 1 shows the source of the samples in the database along with the number of samples for each source. The compiled tensors were generated using the following methods: Electron Back-Scatter Diffraction (EBSD), Ultrasound or Pulse Transmission technique under confining pressure sufficient to close microcracks, X-ray texture goniometry, and texture determination using a universal stage microscope.

Currently, there are 106 samples in this database and the majority are deformed crustal rocks. The majority of the deformed rocks are high grade metamorphic rocks, followed by medium and low grade rocks. There are also a few sedimentary rock samples in the database. Figure 3 illustrates the rock type categorized by the metamorphic grades of the samples in the database.

Figure 2: World map showing locations of the samples in the database.

Source	Number of Samples
Barberini et al. (2007)	2
Barruol and Kern (1996)	2
Barruol and Mainprice (1993)	8
Brownlee et al. (2011)	6
Brownlee et al. (In preparation)	28
Condit et al. (In preparation)	2
Erdman et al. (2013)	24
Ji et al. (2013)	6
Khazanehdari et al. (1998)	1
Rasolofosaon et al. (2000)	2
Takanashi et al. (2001)	4
Tatham et al. (2008)	9
Valcke et al. (2006)	3
Ward et al. (2012)	3
Weiss et al. (1999)	8

Table 1: List of elastic tensor sources and number of samples obtained from each source.

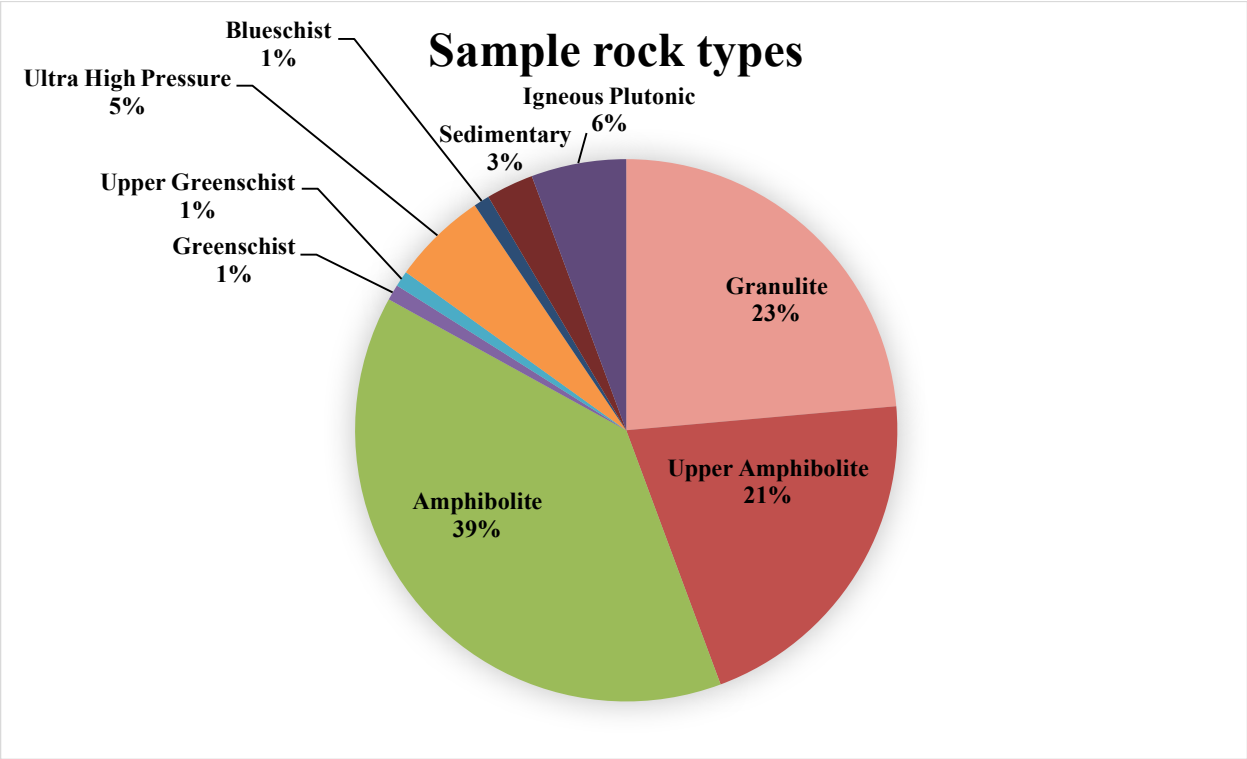

Figure 3: The pie chart shows a representation of the rock types of the samples in the database.

METHODS AND ANALYSIS

Elastic tensor collection

Elastic tensors of rocks were gathered along with their pressure and temperature (P-T) conditions of measurement and fabric formation, mineralogy and bulk composition, density, measurement method, location and rock type. Most of the elastic tensors in the database are the Voigt-Reuss-Hill (VRH) aggregate elastic stiffness approximation from Mainprice's AnisCh5 program (Mainprice, 2007) based on electron backscatter diffraction data.

Elastic tensor decomposition

Elastic tensors were decomposed into different symmetry classes using a method proposed by Browaeys and Chevrot (2004). Each tensor was input into a modified c code from a program for seismic anisotropy calculation in the convective upper mantle. The code was run using Terminal with the mode set to 23. With each tensor input, outputs obtained were percent anisotropy along with a breakdown of the tensor in all the symmetry classes.

Shape factor calculation

η, the shape factor, is an elastic parameter in hexagonal anisotropy used to describe the shape of the velocity ellipsoid between the P-fast and P-slow axis (Porter et al., 2011). The shape factor was calculated using the total hexagonal tensor, which is the sum of isotropic and hexagonal tensor obtained from the tensor decomposition. Using the Love nomenclature, a hexagonal tensor can be described using only 5 coefficients: A, C, F, L and N. The total hexagonal tensor can be expressed using these Love coefficients (Babuska and Cara, 1991):

$$\begin{bmatrix} A & A-2N & F & 0 & 0 & 0 \\ A-2N & A & F & 0 & 0 & 0 \\ F & F & C & 0 & 0 & 0 \\ 0 & 0 & 0 & L & 0 & 0 \\ 0 & 0 & 0 & 0 & L & 0 \\ 0 & 0 & 0 & 0 & 0 & N \end{bmatrix}.$$

The shape factor was calculated using the following formula from Sherrington et al. (2004):

$$\eta = \frac{F}{A-2L}.$$

η can also be expressed in terms of Backus (Backus, 1965) parameters:

$$\eta = \frac{a-3c-2d-2e}{a-b+c-2d-2e}.$$

Kawakatsu et al. (2015) introduced a new fifth parameter that measures the deviance from an elliptical condition of a TI body (Kawakatsu, 2015) called η_K. Kawakatsu et al. (2015) defined η_K as:

$$\eta_K = \frac{F+L}{(A-L)^{1/2}(C-L)^{1/2}}.$$

η_K can also be expressed in terms of Backus parameters:

$$\eta_K = \frac{a-3c-d-e}{(a-b+c-d-e)^{1/2}(a+b+c-d-e)^{1/2}}.$$

a, b, c, d and e calculation

Levin and Park (1997) used the Backus parameters *a*, *b*, *c*, *d* and *e* to define anisotropy. Parameter *a* corresponds to average P velocity, *b* to the percent P anisotropy, *c* to anisotropy ellipsoid variations away from a true ellipsoid, *d* to average S velocity and *e* to percent S anisotropy (Porter et al., 2011). A true ellipsoid is when *c* = 0, therefore, *c* values indicate the ellipticity between the P-fast and P-slow axes. These parameters were calculated using equations from Soukup et al. (2013) which expresses the 5 Love coefficients of a hexagonal tensor to these Backus parameters:

$A = a-b+c$

$C = a+b+c$

$F = a-3c-2(d+e)$

$L = d+e$

$N = d-e$

Hence, I derived equations to calculate these Backus parameters in terms of the Love coefficients:

$a = \frac{1}{4}(F + 2L + 3\frac{C+A}{2})$

$b = \frac{C-A}{2}$

$c = \frac{1}{4}(\frac{C+A}{2} - 2L - F)$

$d = \frac{L+N}{2}$

$$e = \frac{L-N}{2}$$

RESULTS AND DISCUSSION

Figure 4 below shows the variation in percent total anisotropy of the samples in the database. The total anisotropy ranges from 1.27% to 25.47%. This is a result of variation in composition, P-T conditions of fabric formation of the rock samples as well as the degree of mineral alignment within a rock sample.

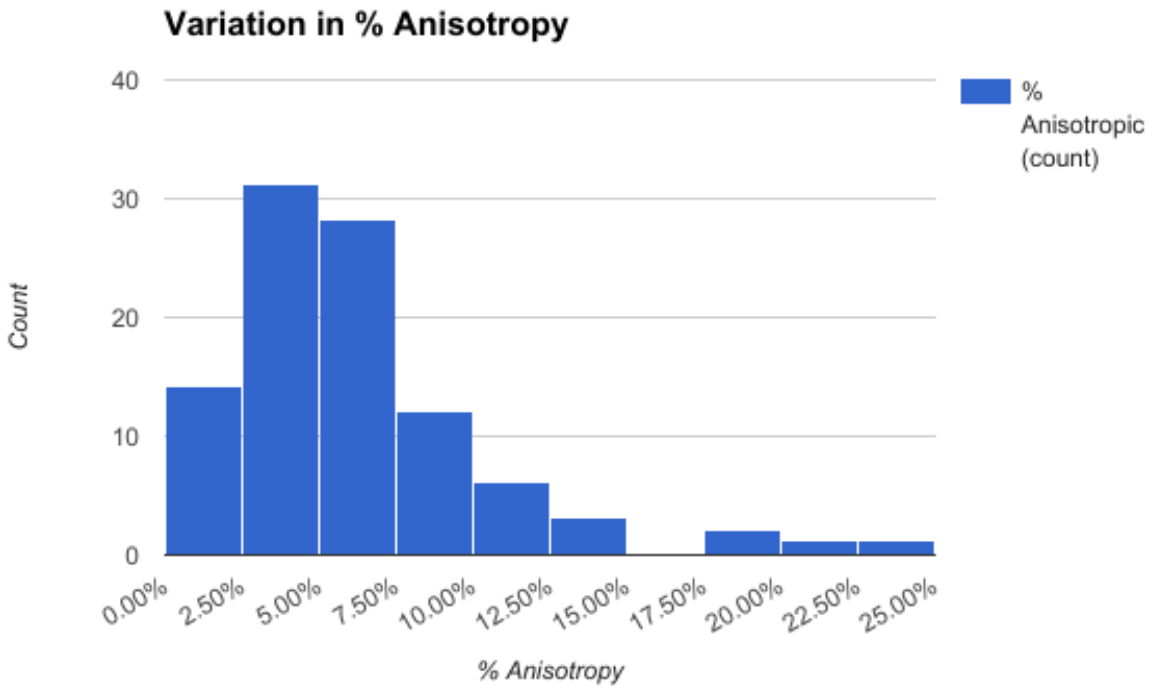

Figure 4: Histogram showing the range in total anisotropy of the rock samples in the database.

Anisotropy symmetry

Each sample in the database exhibits one dominant type of anisotropy symmetry. This can be shown using a stereonet projection. Examples of samples exhibiting dominantly hexagonal, orthorhombic and lower-order symmetry classes of anisotropy are shown below. Note that in the stereonet plots below, the symmetry axis is vertically across the stereonet.

Hexagonal:

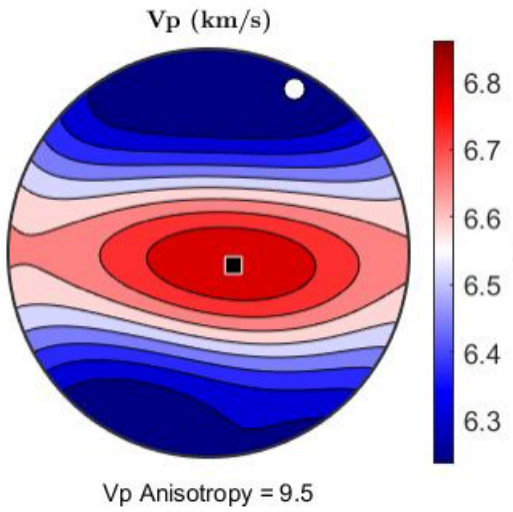

Figure 5: A stereonet projection of sample bt-plg gneiss from Weiss et al. (1999).

Figure 5 is an example of dominantly hexagonal symmetry, which is evident with the presence of two slow Vp poles with a faster Vp region in the middle. This resembles a TI body to which hexagonal symmetry has always been equated (Babuska and Cara, 1991). From the tensor decomposition, this sample is 7.2% hexagonal symmetry with a total anisotropy of 9.8%. The hexagonal symmetry is likely from the alignment of biotite along the foliation plane. However, Ji and Mainprice (1988) states that plagioclase rocks deformed by superplastic deformation mechanism in the lower crust are usually not

anisotropic due to lack of preferred orientation during deformation and the mechanism in fact randomizes pre- existing fabric. Hence, the presence of plagioclase (41.6%) may have significantly reduced the overall rock anisotropy if the rock samples were deformed via this mechanism. This is also supported by the fact that gneiss has a wide range of anisotropy, 2.2 - 21.6%, and this variation is caused by differences in composition and mineral alignment.

Orthorhombic:

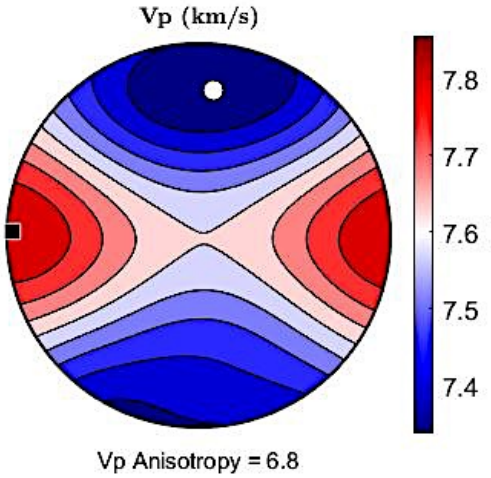

Figure 6: Stereonet projection of sample metapelite I from Weiss et al. (1999).

Figure 6 is an example of a sample exhibiting orthorhombic symmetry. This rock sample contains 21.8% of biotite, 16.2% of quartz, 16.2% of garnet, 15.6 % of potassium feldspar, 14.4% of sillimanite and has no amphibole. Sillimanite has an orthorhombic crystal system. Ji et al. (2015) and Leslie et al. (2015) suggest that sillimanite develops a strong LPO with the fast c axes parallel to the lineation, hence could enhance seismic anisotropy. The orthorhombic symmetry of this sample is likely from a combination of aligned biotite and sillimanite. This sample also contains a significant amount of garnet, an isotropic mineral, which may have reduced the overall magnitude of anisotropy.

Lower-order symmetry class:

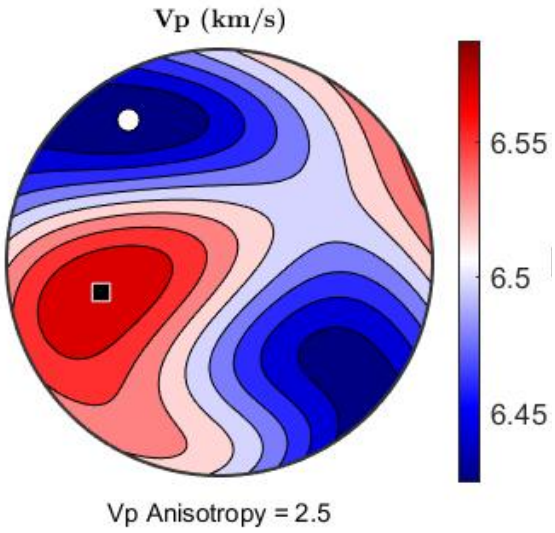

Figure 7: Stereonet projection of sample mqmg-norite from Weiss et al. (1999).

Lower symmetry comprises tetragonal, monoclinic and triclinic symmetry classes. Figure 7 is an example of a rock sample that is not strongly anisotropic and exhibits lower symmetry anisotropy. The plot shows that a lack of significant fast or slow directions. The velocities do not vary much; only about 0.1 km/s, which reflects weak anisotropy.

Mineralogical trends

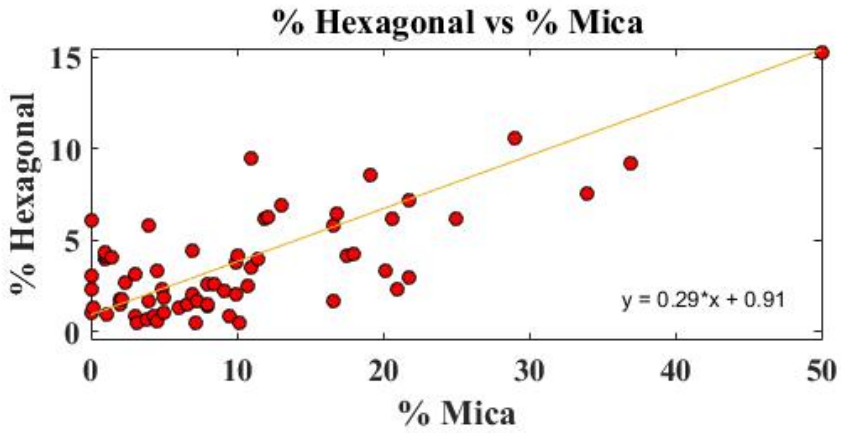

Graph 1: A plot of hexagonal type anisotropy as a function of amount of mica.

Based on Graph 1, there is a strong correlation between the hexagonal component of anisotropy and amount of mica. Increasing mica content in a rock will increase the hexagonal component of anisotropy. This is not surprising and in fact is well expected. Mica, being the most anisotropic mineral, commonly aligns with the fast plane in the foliation plane in deformed rocks (Ward et al., 2012). LPO of anisotropic minerals has been proven to increase seismic anisotropy within a rock body (Dempsey et al. 2011). An equation relating the mica content and hexagonal anisotropy is also given in Graph 1.

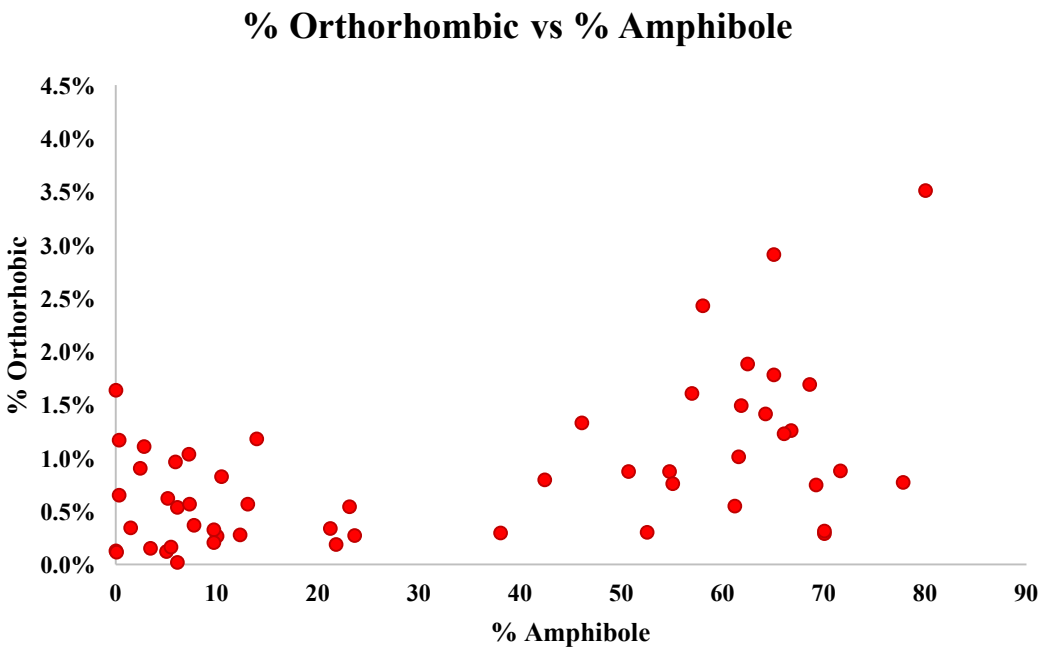

Graph 2: A plot of orthorhombic component of anisotropy as a function of amphibole content in rocks.

Some samples show an increasing trend of orthorhombic component of anisotropy with increasing amount of amphibole as seen in Graph 2. A possible explanation to this is, with higher amounts of amphibole, it is more likely to develop a strong LPO, which then amplifies the anisotropy of the rock sample. The type of amphibole present in these rock samples is hornblende; which has orthorhombic crystal symmetry. This is consistent that the trend with increasing anisotropy is seen with the increasing of orthorhombic component of the anisotropic instead of hexagonal. The presence of aligned amphibole in general will increase the overall rock anisotropy. Hence, though rock samples with less than 20% amphibole can have lower orthorhombic anisotropy, the overall rock anisotropy could be higher. For instance, if a rock sample is dominated by mica, the majority of the anisotropy will be categorized under hexagonal anisotropy. Similar arguments apply for rock samples than contain about 50-70% amphibole but still have low orthorhombic anisotropy. In this case, the anisotropy could be diminished by the presence of minerals such as quartz and garnet, or one axis of the amphiboles may be aligned preferentially while the other two align randomly.

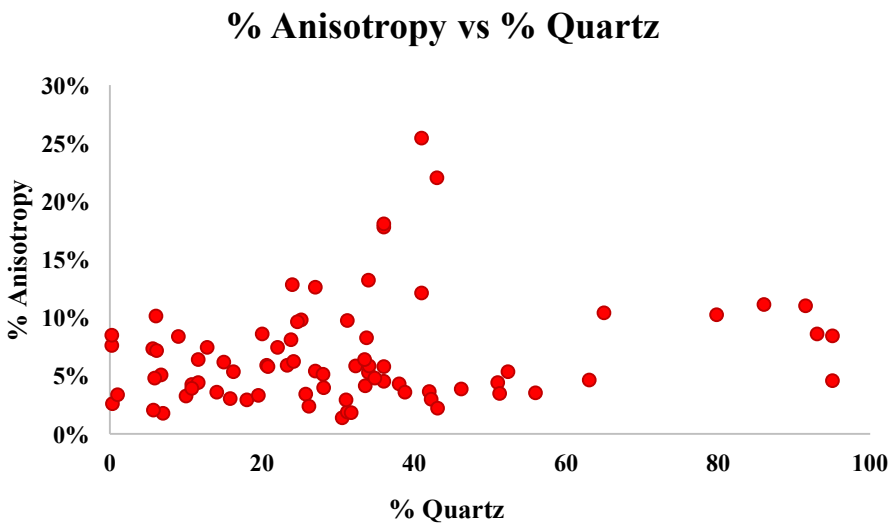

Graph 3: A plot of anisotropy as function of quartz content.

The correlation between quartz content and anisotropy is more complex compared to mica and amphibole. Naturally, quartz crystallizes into trigonal crystal system (if alpha quartz), which is one of the lower symmetries. As shown in Graph 3, rock samples with 0-40% of quartz are bounded between 0-10% of total rock anisotropy. This implies that a quartz dominated rock (~40% of quartz) has anisotropy that is similar to a rock that has little to none (<5%) of quartz. Rocks with quartz is still anisotropic, but the exact relationship between quartz and anisotropy is still ambiguous. Ji et al. (1993) claims that quartz's anisotropy often cancels out with anisotropy of other phases, for example feldspar. Ward et al. (2012) also suggests that interference of quartz in micaceous lithology can significantly reduce the total rock's anisotropy. However, based on Graph 3 and the information present in the database alone, it is hard to say anything conclusive. However, it will be worth looking into specific samples to study the interference of quartz with other minerals within the sample as well as to consider the deformation mechanism of the samples.

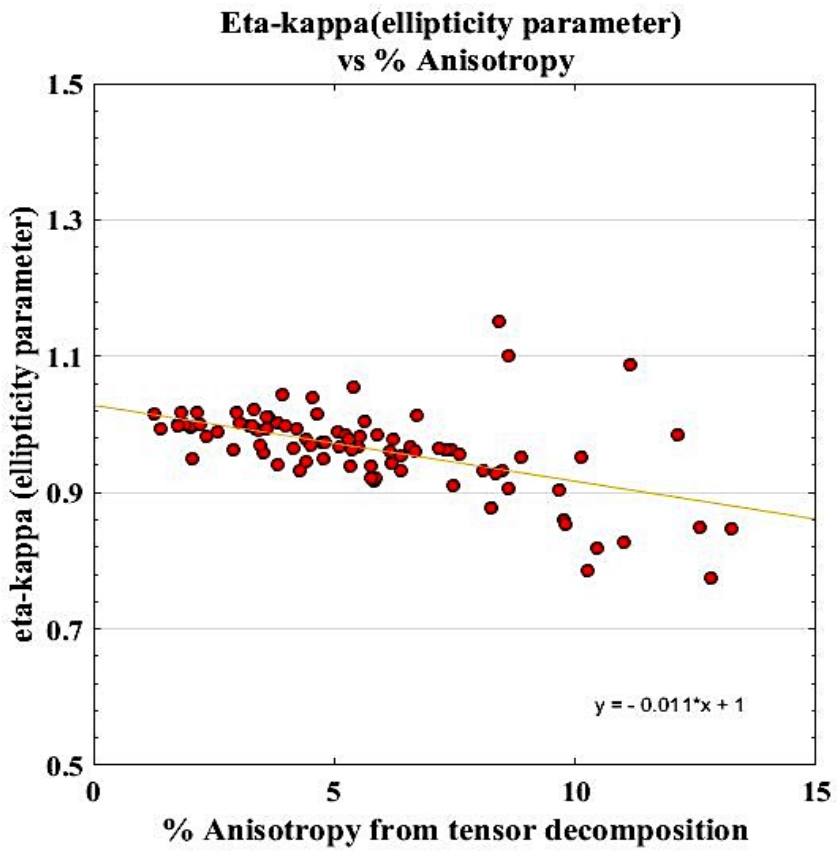

Graph 4: A plot of η_K as a function of percent anisotropy from tensor decomposition.

As shown in Graph 4, the higher the anisotropy of the rock, the lower the η_K value. This is a useful trend that will be beneficial for future studies as past studies have always approximated that $\eta_K = 1$ (indicating a perfect elliptical hexagonal phase velocity) regardless of rock anisotropy. There had been an ambiguity of η_K value being above or below 1 as rocks get more anisotropic in past studies. Xie at al. (2015) used dip angles as a proxy of η that resulted in various solutions for surface wave anisotropy. Hence with the trend shown in Graph 4, an accurate forward modelling could be done by using an ellipticity parameter that is more representative of the rock anisotropy. For instance, for rocks with anisotropy of less than 5%, a suitable η_K value could be 0.96 and 0.92 for rocks with 5-10% of anisotropy.

CONCLUSIONS

This study had built an extensive database that consists of over 100 sample elastic stiffness tensors from published studies in various locations. These rock samples are of various rock type, which is representative of the Earth's lower crust. The elastic tensors were decomposed into symmetry classes using the method proposed by Browaeys and Chevrot (2004). Wide range of total rock anisotropy was observed and this is a result of the variation in rock type and degree of mineral alignment within a rock sample. The total anisotropy of these rock samples ranged from 1.27% to 25.47%. The samples have a dominant type of anisotropy symmetry and this was demonstrated using stereonet projection. Key trends from this study include:

a. Higher mica content correlates to higher hexagonal components of anisotropy.
b. Higher amphibole content correlates to higher orthorhombic components of anisotropy.
c. Rocks with higher anisotropy have lower η_K values, which are lower than 1.

However, the role of quartz in anisotropy is still ambiguous. This study demonstrated that rock with 0-40% of quartz have similar anisotropy. Therefore, it will be worth looking into specific samples to evaluate the interference of quartz with other minerals within the rock sample and the relationship between common deformation mechanisms and anisotropy. This database will be particularly useful for future crustal anisotropy studies that focus on forward modelling.

REFERENCES

Babuska, V., and Cara, M., 1991, Seismic anisotropy in the Earth: Kluwer Academic Publ., Dordrecht.

Bachmann, F., Hielscher, R., and Schaeben, H., 2010, Texture Analysis with MTEX – Free and Open Source Software Toolbox: Solid State Phenomena, v. 160, p. 63–68, doi: 10.4028/www.scientific.net/ssp.160.63.

Backus, G. E., 1965. Possible forms of seismic anisotropy of the uppermost mantle under oceans, J. geophys. Res., 70, 3429–3439, doi:10.1029/JZ070i014p03429.

Bostock, M.G., and Christensen, N.I., 2012, Split from slip and schist: Crustal anisotropy beneath northern Cascadia from non-volcanic tremor: Journal of Geophysical Research: Solid Earth, v. 117, no. B8, doi: 10.1029/2011jb009095.

Browaeys, J.T., and Chevrot, S., 2004, Decomposition of the elastic tensor and geophysical applications: Geophysical Journal International, v. 159, no. 2, p. 667–678, doi: 10.1111/j.1365-246x.2004.02415.x.

Dempsey, E.D., Prior, D.J., Mariani, E., Toy, V.G., and Tatham, D.J., 2011, Mica-controlled anisotropy within mid-to-upper crustal mylonites: an EBSD study of mica fabrics in the Alpine Fault Zone, New Zealand: Geological Society, London, Special Publications, v. 360, no. 1, p. 33–47, doi: 10.1144/sp360.3.

Eaton, D.W., and Jones, A., 2006, Tectonic fabric of the subcontinental lithosphere: Evidence from seismic, magnetotelluric and mechanical anisotropy: Physics of the Earth and Planetary Interiors, v. 158, no. 2-4, p. 85–91, doi: 10.1016/j.pepi.2006.05.005.

Godfrey, N.J., Christensen, N.I., and Okaya, D.A., 2000, Anisotropy of schists: Contribution of crustal anisotropy to active source seismic experiments and shear wave splitting observations: Journal of Geophysical Research: Solid Earth, v. 105, no. B12, p. 27991–28007, doi: 10.1029/2000jb900286.

Hielscher, R., Schaeben, H., 2008. A novel pole figure inversion method: specification of the MTEX algorithm. Journal of Applied Crystallography 41, 1024-1037.

Ji, S. and David, M., 1988, Natural deformation fabrics of plagioclase: implications for slip systems and seismic anisotropy: Tectonophysics, v. 147, no. 1-2, p. 145–163, doi: 10.1016/0040-1951(88)90153-9.

Ji, S., Salisbury, M.H., and Hanmer, S., 1993, Petrofabric, P-wave anisotropy and seismic reflectivity of high-grade tectonites: Tectonophysics, v. 222, no. 2, p. 195–226, doi: 10.1016/0040-1951(93)90049-p.

Ji, S., Shao, T., Michibayashi, K., Oya, S., Satsukawa, T., Wang, Q., Zhao, W., and Salisbury, M.H., 2015, Magnitude and symmetry of seismic anisotropy in mica- and amphibole-bearing metamorphic rocks and implications for tectonic interpretation of seismic data from the southeast Tibetan Plateau: Journal of Geophysical Research: Solid Earth, v. 120, no. 9, p. 6404–6430, doi: 10.1002/2015jb012209.

Kawakatsu, H., 2015, A new fifth parameter for transverse isotropy: Geophysical Journal International, v. 204, no. 1, p. 682–685, doi: 10.1093/gji/ggv479.

Kawakatsu, H., Montagner, J.-P., and Song, T.-R.A., 2015, On DLA's η, in Foulger, G.R., Lustrino, M., and King, S.D., eds., The Interdisciplinary Earth: A Volume in Honor of Don L. Anderson: Geological Society of America Special Paper 514 and American Geophysical Union Special Publication 71, p. 33–38,doi:10.1130/2015.2514(03).

Leslie, S., Mahan, K., Regan, S., Williams, M., and Dumond, G., 2015, Contrasts in sillimanite deformation in felsic tectonites from anhydrous granulite- and hydrous amphibolite-facies shear zones, western Canadian Shield: Journal of Structural Geology, v. 71, p. 112–124, doi: 10.1016/j.jsg.2014.12.002.

Levin, V., and Park, J., 1997, P-SHconversions in a flat-layered medium with anisotropy of arbitrary orientation: Geophysical Journal International, v. 131, no. 2, p. 253–266, doi: 10.1111/j.1365-246x.1997.tb01220.x.

Lloyd, G.E., and Kendall, J.M., 2005, Petrofabric-derived seismic properties of a mylonitic quartz simple shear zone: implications for seismic reflection profiling: Geological Society, London, Special Publications, v. 240, no. 1, p. 75–94, doi: 10.1144/gsl.sp.2005.240.01.07.

Love, A. E. H., 1944. A Treatise on the Mathematical Theory of Elasticity (Dover Publications, New York), pp. 160–162.

Mahan, K., 2006, Retrograde mica in deep crustal granulites: Implications for crustal seismic anisotropy: Geophysical Research Letters, v. 33, no. 24, doi: 10.1029/2006gl028130.

Mainprice, D., 2007, Seismic Anisotropy of the Deep Earth from a Mineral and Rock Physics Perspective: Volume 2: Mineral Physics Treatise on Geophysics, p. 437–491, doi: 10.1016/b978-044452748-6/00045-6.

Margheriti, L., Nostro, C., Amato, A. & Cocco, M., 1997, Seismic anisotropy: an original tool to understand the geodynamic evolution of the Italian peninsula: Annals of Geophysics, v. 40, no. 3.

Porter, R., Zandt, G., and Mcquarrie, N., 2011, Pervasive lower-crustal seismic anisotropy in Southern California: Evidence for underplated schists and active tectonics: Lithosphere, v. 3, no. 3, p. 201–220, doi: 10.1130/l126.1.

Sherrington, H.F., Zandt, G., and Frederiksen, A., 2004, Crustal fabric in the Tibetan Plateau based on waveform inversions for seismic anisotropy parameters: Journal of Geophysical Research: Solid Earth, v. 109, no. B2, doi: 10.1029/2002jb002345.

Soukup, D.J., Odom, R.I., and Park, J., 2013, Modal investigation of elastic anisotropy in shallow-water environments: Anisotropy beyond vertical transverse isotropy: The Journal of the Acoustical Society of America, v. 134, no. 1, p. 185–206, doi: 10.1121/1.4809721.

Tatham, D., Lloyd, G., Butler, R., and Casey, M., 2008, Amphibole and lower crustal seismic properties: Earth and Planetary Science Letters, v. 267, no. 1-2, p. 118–128, doi: 10.1016/j.epsl.2007.11.042.

Ward, D., Mahan, K., and Schulte-Pelkum, V., 2012, Roles of quartz and mica in seismic anisotropy of mylonites: Geophysical Journal International, v. 190, no. 2, p. 1123–1134, doi: 10.1111/j.1365-246x.2012.05528.x.

Weiss, T., Siegesmund, S., Rabbel, W., Bohlen, T., and Pohl, M., 1999, Seismic Velocities and Anisotropy of the Lower Continental Crust: A Review: Seismic Exploration of the Deep Continental Crust, p. 97–122, doi: 10.1007/978-3-0348-8670-3_6.

Xie, J., Ritzwoller, M.H., Brownlee, S.J., and Hacker, B.R., 2015, Inferring the oriented elastic tensor from surface wave observations: preliminary application across the western United States: Geophysical Journal International, v. 201, no. 2, p. 996–1019, doi: 10.1093/gji/ggv054.

APPENDIX A

LIST OF CRUSTAL ELASTIC TENSOR SOURCES

Barberini, V., Burlini, L., and Zappone, A., 2007, Elastic properties, fabric and seismic anisotropy of amphibolites and their contribution to the lower crust reflectivity: Tectonophysics, v. 445, no. 3-4, p. 227–244, doi: 10.1016/j.tecto.2007.08.017.

Barruol, G., and Mainprice, D., 1993, 3-D seismic velocities calculated from lattice-preferred orientation and reflectivity of a lower crustal section: examples of the Val Sesia section (Ivrea zone, northern Italy): Geophysical Journal International, v. 115, no. 3, p. 1169–1188, doi: 10.1111/j.1365-246x.1993.tb01519.x.

Barruol, G., and Kern, H., 1996, Seismic anisotropy and shear-wave splitting in lower-crustal and upper-mantle rocks from the Ivrea Zone—experimental and calculated data: Physics of the Earth and Planetary Interiors, v. 95, no. 3-4, p. 175–194, doi: 10.1016/0031-9201(95)03124-3.

Brownlee, S.J., Hacker, B.R., Salisbury, M., Seward, G., Little, T.A., Baldwin, S.L., and Abers, G.A., 2011, Predicted velocity and density structure of the exhuming Papua New Guinea ultrahigh-pressure terrane: Journal of Geophysical Research, v. 116, no. B8, doi: 10.1029/2011jb008195.

Brownlee et al., in preparation.

Condit et al., in preparation.

Erdman, M.E., Hacker, B.R., Zandt, G., and Seward, G., 2013, Seismic anisotropy of the crust: electron-backscatter diffraction measurements from the Basin and Range: Geophysical Journal International, v. 195, no. 2, p. 1211–1229, doi: 10.1093/gji/ggt287.

Ji, S., Shao, T., Michibayashi, K., Long, C., Wang, Q., Kondo, Y., Zhao, W., Wang, H., and Salisbury, M.H., 2013, A new calibration of seismic velocities, anisotropy, fabrics, and elastic moduli of amphibole-rich rocks: Journal of Geophysical Research: Solid Earth, v. 118, no. 9, p. 4699–4728, doi: 10.1002/jgrb.50352.

Khazanehdari, J., Rutter, E., Casey, M., and Burlini, L., 1998, The role of crystallographic fabric in the generation of seismic anisotropy and reflectivity of high strain zones in calcite rocks: Journal of Structural Geology, v. 20, no. 2-3, p. 293–299, doi: 10.1016/s0191-8141(97)00061-8.

Rasolofosaon, P.N.J., Rabbel, W., Siegesmund, S., and Vollbrecht, A., 2000, Characterization of crack distribution: fabric analysis versus ultrasonic inversion: Geophysical Journal International, v. 141, no. 2, p. 413–424, doi: 10.1046/j.1365-246x.2000.00093.x.

Takanashi, M., Nishizawa, O., Kanagawa, K., and Yasunaga, K., 2001, Laboratory measurements of elastic anisotropy parameters for the exposed crustal rocks from the Hidaka Metamorphic Belt, Central

Hokkaido, Japan: Geophysical Journal International, v. 145, no. 1, p. 33–47, doi: 10.1111/j.1365-246x.2001.00332.x.

Tatham, D., Lloyd, G., Butler, R., and Casey, M., 2008, Amphibole and lower crustal seismic properties: Earth and Planetary Science Letters, v. 267, no. 1-2, p. 118–128, doi: 10.1016/j.epsl.2007.11.042.

Valcke, S.L.A., Casey, M., Lloyd, G.E., Kendall, J.-M., and Fisher, Q.J., 2006, Lattice preferred orientation and seismic anisotropy in sedimentary rocks: Geophysical Journal International, v. 166, no. 2, p. 652–666, doi: 10.1111/j.1365-246x.2006.02987.x.

Ward, D., Mahan, K., and Schulte-Pelkum, V., 2012, Roles of quartz and mica in seismic anisotropy of mylonites: Geophysical Journal International, v. 190, no. 2, p. 1123–1134, doi: 10.1111/j.1365-246x.2012.05528.x.

Weiss, T., Siegesmund, S., Rabbel, W., Bohlen, T., and Pohl, M., 1999, Seismic Velocities and Anisotropy of the Lower Continental Crust: A Review: Seismic Exploration of the Deep Continental Crust, p. 97–122, doi: 10.1007/978-3-0348-8670-3_6.